

Intranight Optical Variability of Radio-Quiet Weak Emission Line Quasars-III

Parveen Kumar^{1*}, Gopal-Krishna², Hum Chand¹

¹*Aryabhata Research Institute of Observational Sciences (ARIES), Manora Peak, Nainital, 263002 India,*

²*Centre for Excellence in Basic Sciences (CBS), University of Mumbai campus (Kalina), Mumbai 400098, India*

Accepted —. Received —; in original form —

ABSTRACT

This is continuation of our programme to search for the elusive radio-quiet BL Lacs, by carrying out a systematic search for intranight optical variability (INOV) in a subset of ‘weak-line quasars’ which are already designated as ‘high-confidence BL Lac candidate’ and are also known to be radio-quiet. For 6 such radio-quiet weak-line quasars (RQWLQs), we present here new INOV observations taken in 11 sessions of duration >3 hours each. Combining these data with our previously published INOV monitoring of RQWLQs in 19 sessions yields INOV observations for a set of 15 RQWLQs monitored in 30 sessions, each lasting more than 3 hours. The 30 differential light curves, thus obtained for the 15 RQWLQs, were subjected to a statistical analysis using the F–test, and the deduced INOV characteristics of the RQWLQs then compared with those published recently for several prominent AGN classes, also applying the F–test. From our existing INOV observations, there is a hint that RQWLQs in our sample show a significantly higher INOV duty cycle than radio-quiet quasars and radio lobe-dominated quasars. Two sessions when we have detected strong (blazar-like) INOV for RQWLQs are pointed out, and these two RQWLQs are therefore the best known candidates for radio-quiet BL Lacs, deserving to be pursued. For a proper comparison with the INOV properties already established for (brighter) members of several prominent classes of AGN, a factor of 2 – 3 improvement in the INOV detection threshold for the RQWLQs is needed and it would be very interesting to check if that would yield a significantly higher estimate for INOV duty cycle than is found here.

Key words: galaxies: active – galaxies: photometry – galaxies: jet – quasars: general – (galaxies:) BL Lacertae objects: general – (galaxies:) quasars: emission lines

1 INTRODUCTION

Flux variations at all energy bands is a well known characteristic of active galactic nuclei (AGN) (e.g. see [Urry & Padovani 1995](#)). Optical flux variation on hour-like time scale, which is commonly known as ‘intranight optical variability’ (INOV), has emerged as a useful probe of AGN ([Wagner & Witzel 1995](#); [Ulrich et al. 1997](#); [Wiita 2006](#)). The past two decades have witnessed a large number of INOV studies covering different classes of AGN, in order to study the physical processes underlying this phenomenon occurring in the different AGN classes ([Miller et al. 1989](#); [Heidt & Wagner 1996](#); [Carini et al. 1990, 1991, 1992, 2007](#); [Carini & Miller 1992](#); [Gopal-Krishna et al. 1995, 1993](#); [Stalin et al. 2004b](#); [Gupta & Joshi 2005](#); [Joshi et al. 2011](#); [Joshi & Chand 2013](#);

[Goyal et al. 2013](#); [Chand et al. 2014](#); [de Diego 2014](#)). These studies have led to theoretical models for INOV (e.g. see [Ulrich et al. 1997](#); [Czerny et al. 2008](#); [Wiita 2006](#)). For instance, in blazars, where pronounced INOV is observed, the cause could be turbulence or localised particle acceleration events within the non-thermal plasma flowing in a relativistic jet (e.g., [Wagner & Witzel 1995](#); [Gopal-Krishna et al. 2003](#); [Singal & Gopal-Krishna 1985](#)). On the other hand, in the case of radio-quiet quasars (RQQSOs) flares occurring in the accretion disc might also play a significant if not dominant, role in causing the INOV ([Mangalam & Wiita 1993](#)). In gamma-ray-loud narrow-line Seyfert1 galaxies, the detection of INOV on hour-like or shorter time scale points to the presence of non-thermal jets with large Doppler factors ([Paliya et al. 2013](#)). Hence, INOV studies of different classes of AGN can play a useful role in improving the understanding of the AGN physics.

Weak emission line quasars (WLQs) is a relatively recently discovered and rather enigmatic class of AGN (e.g.,

* E-mail: parveen@aries.res.in (PK); gopaltani@gmail.com (GK); hum@aries.res.in (HC)

Smith et al. 2007; Plotkin et al. 2010; Heidt & Nilsson 2011). They exhibit abnormally weak broad emission-lines (i.e, rest-frame $EW < 15.4\text{\AA}$ for the Ly+NV emission-line complex, Diamond-Stanic et al. 2009). The physical cause for the abnormally weak line emission continues to be debated, as summarized in the previous papers of this series (Gopal-Krishna et al. 2013; Chand et al. 2014, hereinafter Paper I & Paper II). It may be recalled that according to the currently prevailing view, the two sub-classes of the most active AGN, called blazars, are BL Lac objects (BLOs) and Highly-Polarized-Quasars (HPQs) which differ primarily in the prominence of emission lines in the optical spectrum. But, whereas HPQs have an abundant population of (usually weakly polarized) radio-quiet counterparts (the RQQs), searches for radio-quiet analogs of BLOs have so far remained unsuccessful, even probing the radio-quiet subset of WLQs (RQWLQs) as possible candidates (e.g., Jannuzi et al. 1993; Londish et al. 2004).

The explanations proposed for the WLQs basically fall in two categories. One possible cause of the abnormality is the high mass of the central BH ($M_{BH} > 3 \times 10^9 M_{\odot}$) which can result in an accretion disk too cold to emit strongly the ionizing UV photons, even when its optical output is high (Laor & Davis 2011; also, Plotkin et al. 2010). Alternatively, the covering factor of the broad-line region (BLR) in WLQs could be at least an order-of-magnitude smaller compared to the normal QSOs (e.g., Nikolajuk & Walter 2012). An extreme version of this scenario is that in WLQs the accretion disk is relatively recently established and hence a significant BLR is yet to develop (Hryniewicz et al. 2010; Liu & Zhang 2011). Conceivably, a poor BLR could also result from the weakness of the radiation pressure driven wind when the AGN is operating at an exceptionally low accretion rate ($< 10^{-2}$ to $10^{-3} \dot{M}_{Edd}$) (Nicastro et al. 2003; also, Elitzur & Ho 2009).

While the above mechanisms may well operate commonly, a small fraction of RQWLQs may nonetheless turn out to be the radio-quiet counterparts of BL Lacs, such that the relativistic jet itself is radio-quiet. In order to pursue this interesting question, we started in 2012 an observational programme aimed at determining the INOV characteristics of RQWLQs (Papers I and II). In the present work (Paper III), we report the INOV results for 6 of the RQWLQs which we monitored on 11 nights. This paper is organized as follows. Section 2 describes our RQWLQ sample. Observations and data reduction procedures are described in Section 3. Details of our statistical analysis are presented in Section 4, followed by a brief discussion of the results in Section 5.

2 OBSERVATIONS AND DATA REDUCTION

2.1 The sample of radio-quiet WLQs

Our sample for INOV monitoring (Table 1) was derived from the list of 86 radio-quiet WLQs published in Table 6 of Plotkin et al. (2010), based on the SDSS Data Release 7 (DR-7, Abazajian et al. 2009). Out of that list, we included in our sample all 19 objects which are brighter than $R \sim 18.5$ and are classified therein as ‘high-confidence BL Lac candidate’ (e.g., see Paper I and Paper II). Recently we have noticed that their classification as ‘high-confidence

BL Lac candidate’, is not fully secure, since it lacks a check for proper motion.

In fact, one of these 19 WLQs, J090107.64+384658.8, has already been argued to be galactic, based on its large proper motion of $62.3 \pm 10.9 \text{mas/yr}$ (Wu et al. 2012). In view of this, we have carried out a search for proper motion data for our set of 19 WLQs, using the latest USNO catalog (Monet et al. 2003) and the values are reproduced in the last column of Table 1. From this table, seven members of our set of 19 RQWLQs are seen to have a non-zero proper motion. However, for three of them (viz. J110938+373611, J140710+241853 and J161245+511817), the quoted proper motion is not significant ($< 2.5\sigma$), making their galactic classification uncertain (the choice of rms threshold is consistent with Londish et al. 2004). This is further corroborated by the fact that, based on a multi-wavelength SED analysis, Wu et al. (2012) have confirmed extragalactic nature for the WLQ J110938+373611 for which USNO proper motion is $10.8 \pm 4.5 \text{mas/yr}$. Likewise, for J140710+241853 and J161245+511817, non-zero redshifts have been confirmed by Hewett & Wild (2010). Therefore, we have retained these three sources in our RQWLQ sample, and removed the remaining four sources for which proper motion is detected above 2.5σ (these sources are marked with †) in Table 1). Thus, the proper motion check reduces our sample from 19 to 15 RQWLQs and these can be regarded as bona-fide ‘high-confidence BL Lac candidates’. New observations of 6 out of these 15 RQWLQs (marked by asterisk (*) in Table 1) are reported in the present work, based on 11 monitoring sessions. Note that one of the 4 excluded sources is J121929+471522 for which INOV detection with an amplitude of $\sim 7\%$ over a few hours was reported in Paper I.

3 OBSERVATIONS AND DATA REDUCTION

3.1 Photometric Monitoring Observations

The programme to determine the INOV properties of RQWLQs, initially reported in Paper I, has been primarily carried out using the 1.3-m Devasthal Fast Optical Telescope (DFOT) of the Aryabhata Research Institute of Observational Sciences (ARIES) located at Devasthal, India (Sagar et al. 2011). We have also used the 1.04-m Sampurnanand and IUCAA Girawali Observatory (IGO) telescopes for optical monitoring of a few of these sources (Paper I). The entire monitoring was done in the r band and each time a given RQWLQ was monitored continuously for not less than 3.5 hours, except in case of J140710.26+241853.6 when the duration was a bit shorter (3.0 hours, Table 4). DFOT is a fast beam (f/4) optical telescope with a pointing accuracy better than 10 arcsec RMS. It is equipped with a $2K \times 2K$ Peltier-cooled Andor CCD camera having a pixel size of 13.5 micron and a plate scale of 0.54 arcsec per pixel. The CCD covers a field of view of 18 arcmin on the sky and is read out with 31 kHz and 1000 kHz speeds, with the corresponding system RMS noise of 2.5, 7 e- and a gain of 0.7, 2 e-/Analog to Digital Unit (ADU), respectively. The CCD used in our observations was cooled thermo-electrically to -85degC . The duration of each science frame was about 5–7 minutes, yielding a typical SNR above 25–30. The FWHM

Table 1. The set of 19 ‘RQWLQs’ initially selected for our INOV programme^a.

IAU Name ^a	R.A.(J2000) (h m s)	Dec(J2000) (° ′ ″)	<i>R</i> (mag)	<i>z</i>	PM mas/yr
(1)	(2)	(3)	(4)	(5)	(6)
J081250.79+522531.05*	08 12 50.80	+52 25 31	18.30	1.152	00
J084424.20+124546.00	08 44 24.20	+12 45 46	18.28	2.466	00
J090107.60+384659.00 [†]	09 01 07.60	+38 46 59	18.21	1.329	62.3±10.8
J090843.25+285229.80*	09 08 43.25	+28 52 29	18.55	0.930	00
J101353.45+492757.99	10 13 53.45	+49 27 57	18.40	1.635	00
J110938.50+373611.60	11 09 38.50	+37 36 11	18.72	0.397	10.8±4.5
J111401.31+222211.50 [†]	11 14 01.31	+22 22 11	18.77	2.121	10.2±2.0
J115637.02+184856.50	11 56 37.02	+18 48 56	18.42	1.956	00
J121929.50+471522.00 [†]	12 19 29.50	+47 15 22	17.66	1.336	112.1±3.6
J125219.50+264053.00	12 52 19.50	+26 40 53	17.94	1.292	00
J134601.29+585820.10*	13 46 01.29	+58 58 20	17.73	1.22	00
J140710.26+241853.60*	14 07 10.26	+24 18 53	18.49	1.662	12.0±5.1
J141200.04+634414.90*	14 12 00.04	+63 44 14	17.97	0.068	00
J142943.60+385932.00	14 29 43.60	+38 59 32	17.56	0.925	00
J153044.10+231014.00	15 30 44.10	+23 10 14	17.32	1.040	00
J160410.22+432614.70*	16 04 10.22	+43 26 14	18.04	1.568	00
J161245.68+511817.31	16 12 45.68	+51 18 17	17.70	1.595	2.0±2.0
J212416.05−074129.90	21 24 16.05	+07 41 29	18.29	1.402	00
J224749.56+134250.00 [†]	22 47 49.56	+13 42 50	18.53	1.179	14.1±3.6

^a Result for the sources marked by * are reported in this paper. Although all these sources are classified as ‘high-confidence BL Lac candidate’ in Plotkin et al. (2010), the 4 sources marked by [†] are probably galactic, due to their significant proper motion.

of the seeing disk during our observing was generally ~ 2.5 arcsec.

In our sample selection process, care was taken to identify at least two, but usually more, comparison stars on the CCD frame that were within about 1 mag of the target RQWLQ. This allowed us to pin down and discount any comparison stars which showed variability during our observations, thus permitting a reliable differential photometry of the RQWLQ monitored.

3.2 Data Reduction

The pre-processing work on the raw images (bias subtraction, flat-fielding, cosmic-ray removal and trimming) was carried out using the standard tasks in the Image Reduction and Analysis Facility IRAF¹. The instrumental magnitudes of the RQWLQs and their comparison stars in the image frames were determined by aperture photometry technique (Stetson 1992, 1987), using the Dominion Astronomical Observatory Photometry II (DAOPHOT II)².

The aperture photometry was carried out for four values of aperture radii, $1 \times \text{FWHM}$, $2 \times \text{FWHM}$, $3 \times \text{FWHM}$ and $4 \times \text{FWHM}$. Seeing disk radius ($=\text{FWHM}/2$) for each CCD frame was determined by averaging over 5 adequately bright stars present within each CCD frame. While the photometric data using the different aperture radii were found to be in good agreement, the best S/N was almost always found with

aperture radius of $2 \times \text{FWHM}$. Hence, we adopted it for our final analysis.

To derive the Differential Light Curves (DLCs) of a given target RQWLQ, we selected two steady comparison stars present within the CCD frames, on the basis of their proximity to the target source, both in location and apparent magnitude. Coordinates of the comparison stars selected for each RQLWQ are given in Table 2. The $g - r$ color difference for our ‘quasar-star’ and ‘star-star’ pairs is always < 1.5 , with a median value of 0.56 (column 7, Table 2). Detailed analyses by Carini et al. (1992) and Stalin et al. (2004a) have shown that color difference of this magnitude should produce a negligible effect on the DLCs as the atmospheric attenuation varies over a monitoring session.

Since the selected comparison stars are non-varying, as judged from the steadiness of the star-star DLCs, any sharp fluctuation confined to a single data point was taken to arise from improper removal of cosmic rays, or some unknown instrumental effect, and such outlier data points (deviating by more than 3σ from the mean) were removed from the affected DLCs, by applying a mean clip algorithm. In practice, such outliers were quite rare and never exceeded two data points for any DLC, as displayed in Figure 1.

4 STATISTICAL ANALYSIS OF DLCS

For checking the presence of INOV in a DLC, C-statistic (Jang & Miller 1997) has been the most commonly used test. Although the ‘one-way analysis of variance’ (ANOVA) is the most powerful test for this purpose, it requires a longer data train than is usually present in the

¹ IMAGE REDUCTION AND ANALYSIS FACILITY
([HTTP://IRAF.NOAO.EDU/](http://iraf.noao.edu/))

² DOMINION ASTROPHYSICAL OBSERVATORY PHOTOMETRY

Table 2. Basic parameters and observing log for the 6 RQWLQs and their chosen comparison stars (S1,S2).

IAU Name	Date	R.A.(J2000)	Dec.(J2000)	g	r	$g-r$
(1)	dd.mm.yy	(h m s)	($^{\circ}$ ' ")	(mag)	(mag)	(mag)
	(2)	(3)	(4)	(5)	(6)	(7)
J081250.79+522531.0	01.01.2014	08 12 50.79	+52 25 31.0	18.30	18.05	0.25
S1		08 13 58.01	+52 25 21.9	18.41	17.93	0.48
S2		08 13 20.70	+52 23 27.8	18.36	17.80	0.56
J081250.79+522531.0	02.01.2014	08 12 50.79	+52 25 31.0	18.30	18.05	0.25
S1		08 13 20.70	+52 23 27.8	18.36	17.80	0.56
S2		08 13 52.52	+52 27 01.0	18.99	17.79	1.20
J090843.25+285229.8	01.02.2014	09 08 43.25	+28 52 29.8	18.55	18.50	0.05
S1		09 09 00.07	+28 56 48.4	19.24	18.22	1.02
S2		09 08 58.83	+28 55 38.9	18.93	17.93	1.00
J090843.25+285229.8	02.02.2014	09 08 43.25	+28 52 29.8	18.55	18.50	0.05
S1		09 09 05.04	+28 57 03.9	18.89	17.86	1.03
S2		09 08 27.93	+28 44 41.9	18.10	17.73	0.37
J090843.25+285229.8	01.04.2014	09 08 43.25	+28 52 29.8	18.55	18.50	0.05
S1		09 08 32.43	+28 50 38.5	18.85	18.07	0.78
S2		09 08 41.76	+28 52 17.5	19.31	18.85	1.46
J090843.25+285229.8	03.04.2014	09 08 43.25	+28 52 29.8	18.55	18.50	0.05
S1		09 08 15.05	+28 48 39.6	18.27	17.83	0.44
S2		09 08 49.14	+28 45 42.2	18.26	17.74	0.52
J134601.29+585820.1	01.04.2014	13 46 01.29	+58 58 20.1	17.96	17.74	0.22
S1		13 46 32.38	+58 50 39.1	18.54	17.18	1.36
S2		13 45 46.99	+59 01 59.5	17.65	17.12	0.53
J140710.26+241853.6	03.05.2014	14 07 10.26	+24 18 53.6	18.70	18.47	0.23
S1		14 07 30.89	+24 14 17.7	18.63	17.18	1.45
S2		14 06 50.43	+24 10 48.3	18.54	17.19	1.35
J141200.04+634414.9	04.05.2014	14 12 00.04	+63 44 14.9	17.77	17.05	0.72
S1		14 12 03.97	+63 43 05.9	17.63	17.11	0.52
S2		14 12 35.80	+63 37 16.1	17.53	16.94	0.59
J160410.22+432614.7	05.05.2014	16 04 10.22	+43 26 14.7	18.22	18.04	0.18
S1		16 04 10.58	+43 27 15.1	18.29	17.46	0.83
S2		16 04 48.24	+43 23 31.4	18.42	17.36	1.06
J160410.22+432614.7	30.05.2014	16 04 10.22	+43 26 14.7	18.22	18.04	0.18
S1		16 04 15.97	+43 19 17.7	18.75	17.66	1.09
S2		16 04 48.24	+43 23 31.4	18.42	17.36	1.06

Table 3. Observational details and INOV results for the set of 6 RQWLQs monitored in 11 sessions (present work).

RQWLQ	Date	T	N	F-test values	INOV status ^a	$\sqrt{\langle\sigma_{i,err}^2\rangle}$	INOV amplitude
(1)	dd.mm.yyyy	hr	(4)	F_1^η, F_2^η	F_η -test	(q-s)	ψ_1 (%), ψ_2 (%)
	(2)	(3)	(4)	(5)	(6)	(7)	(8)
J081250.79+522531.0	01.01.2014	3.59	31	0.43, 0.73	NV, NV	0.02	3.43, 5.74
J081250.79+522531.0	02.01.2014	3.46	30	0.38, 0.43	NV, NV	0.02	2.98, 4.40
J090843.25+285229.8	01.02.2014	4.69	39	0.46, 0.56	NV, NV	0.03	8.29, 7.88
J090843.25+285229.8	02.02.2014	4.29	36	0.62, 0.58	NV, NV	0.07	30.39, 23.85
J090843.25+285229.8	01.04.2014	4.92	42	0.50, 0.71	NV, NV	0.03	6.23, 8.95
J090843.25+285229.8	03.04.2014	4.30	37	0.58, 0.73	NV, NV	0.03	10.82, 11.46
J134601.29+585820.1	01.04.2014	4.21	36	0.48, 0.51	NV, NV	0.02	4.18, 4.52
J140710.26+241853.6	03.05.2014	3.00	23	4.19, 4.37	V, V	0.05	37.24, 36.73
J141200.04+634414.9	04.05.2014	4.56	37	0.40, 0.26	NV, NV	0.04	10.28, 5.75
J160410.22+432614.7	05.05.2014	4.62	38	1.01, 1.01	NV, NV	0.04	26.05, 24.60
J160410.22+432614.7	30.05.2014	4.32	37	1.08, 1.11	NV, NV	0.04	17.61, 15.52

^a V=variable, i.e., confidence level ≥ 0.99 ; PV=probable variable, i.e., 0.95 – 0.99 confidence level; NV=non-variable, i.e., confidence level < 0.95 . Variability status inferred, F^η values and INOV peak-to-peak amplitudes(ψ) using the quasar-star1 and quasar-star2 DLCs are separated by a comma.

Table 4. Observational details and INOV results for our entire set of 15 RQWLQs, covered in 30 monitoring sessions.

RQWLQ	Date	T	N	F-test values	INOV status ^a	$\sqrt{\langle\sigma_{i,err}^2\rangle}$	INOV amplitude	References
(1)	dd.mm.yyyy	hr	(4)	F_1^η, F_2^η	F_η -test	(7)	ψ_1 (%), ψ_2 (%)	(9)
J081250.79+522530.9	23.01.2012	5.70	13	0.77, 0.59	NV, NV	0.01	3.03, 1.94	Paper I
J084424.24+124546.5	26.02.2012	4.28	17	0.65, 0.63	NV, NV	0.02	4.49, 3.49	Paper I
J125219.47+264053.9	25.02.2012	2.23	09	0.24, 0.37	NV, NV	0.01	0.36, 1.39	Paper I
J125219.47+264053.9	23.03.2012	3.45	09	0.98, 1.02	NV, NV	0.02	3.93, 3.87	Paper I
J125219.47+264053.9	19.05.2012	3.81	15	0.52, 0.54	NV, NV	0.02	3.43, 3.76	Paper I
J142943.64+385932.2	27.02.2012	3.76	18	0.46, 1.41	NV, NV	0.01	3.49, 4.58	Paper I
J153044.07+231013.5	27.04.2012	4.07	20	2.13, 1.48	NV, NV	0.01	5.46, 3.81	Paper I
J153044.07+231013.5	19.05.2012	3.21	13	0.67, 0.58	NV, NV	0.02	4.19, 4.02	Paper I
J161245.68+511817.3	18.05.2012	4.03	16	0.44, 0.44	NV, NV	0.03	4.02, 3.87	Paper I
J081250.79+522531.0	12.11.2012	4.49	50	0.44, 0.78	NV, NV	0.04	10.70, 12.91	Paper II
J084424.24+124546.5	13.11.2012	3.93	25	0.23, 0.33	NV, NV	0.04	3.91, 5.66	Paper II
J084424.24+124546.5	04.11.2013	3.23	38	0.45, 0.50	NV, NV	0.02	6.15, 6.95	Paper II
J090843.25+285229.8	09.02.2013	3.90	32	0.33, 0.44	NV, NV	0.04	5.06, 8.90	Paper II
J090843.25+285229.8	10.02.2013	4.02	33	3.01, 3.14	V, V	0.04	31.73, 30.20	Paper II
J101353.45+492757.9	01.01.2014	4.43	37	1.96, 1.58	PV, NV	0.02	12.79, 11.07	Paper II
J101353.45+492757.9	02.01.2014	4.58	32	1.10, 0.78	NV, NV	0.02	10.68, 7.31	Paper II
J110938.50+373611.6	10.02.2013	4.43	36	0.54, 0.52	NV, NV	0.03	9.89, 9.14	Paper II
J115637.02+184856.5	15.01.2013	5.05	41	0.59, 0.74	NV, NV	0.03	7.60, 7.97	Paper II
J212416.05-074129.9	12.11.2012	3.40	37	1.08, 1.07	NV, NV	0.07	33.33, 35.20	Paper II
J081250.79+522531.0	01.01.2014	3.59	31	0.43, 0.73	NV, NV	0.02	3.43, 5.74	Present work
J081250.79+522531.0	02.01.2014	3.46	30	0.38, 0.43	NV, NV	0.02	2.98, 4.40	Present work
J090843.25+285229.8	01.02.2014	4.69	39	0.46, 0.56	NV, NV	0.03	8.29, 7.88	Present work
J090843.25+285229.8	02.02.2014	4.29	36	0.62, 0.58	NV, NV	0.07	30.39, 23.85	Present work
J090843.25+285229.8	01.04.2014	4.92	42	0.50, 0.71	NV, NV	0.03	6.23, 8.95	Present work
J090843.25+285229.8	03.04.2014	4.30	37	0.58, 0.73	NV, NV	0.03	10.82, 11.46	Present work
J134601.29+585820.1	01.04.2014	4.21	36	0.48, 0.51	NV, NV	0.02	4.18, 4.52	Present work
J140710.26+241853.6	03.05.2014	3.00	23	4.19, 4.37	V, V	0.05	37.24, 36.73	Present work
J141200.04+634414.9	04.05.2014	4.56	37	0.40, 0.26	NV, NV	0.04	10.28, 5.75	Present work
J160410.22+432614.7	05.05.2014	4.62	38	1.01, 1.01	NV, NV	0.04	26.05, 24.60	Present work
J160410.22+432614.7	30.05.2014	4.32	37	1.08, 1.11	NV, NV	0.04	17.61, 15.52	Present work

^a V=variable, i.e., confidence level ≥ 0.99 ; PV=probable variable, i.e., 0.95 – 0.99 confidence level; NV=non-variable, i.e., confidence level < 0.95 . Variability status, F^η values and the INOV amplitudes(ψ) derived using quasar-star1 and quasar-star2 DLCs are separated by a comma.

available DLCs (de Diego 2010). In our analysis we have not used the C-test since, as pointed out by de Diego (2010), the C-statistics, which is based on ratio of standard deviations is not a reliable test for INOV. This is because : (i) C is not a linear operator (ii) the commonly adopted critical value ($C = 2.576$) is too conservative (de Diego 2010). At the same time, the ANOVA test was not found feasible since most of our DLCs contains no more than 40 data points. Therefore, we have based our statistical analysis on the F-test which employs the ratio of variances as, $F = \text{variance}(\text{observed})/\text{variance}(\text{expected})$ (de Diego 2010), with its two versions : (i) the standard F -test (hereafter F^η -test, Goyal et al. (2012)) and (ii) scaled F-test (hereafter F^κ -test, Joshi et al. (2011)). F^κ -test is mainly used in cases when a large magnitude difference is present between the target object and the available comparison stars (Joshi et al. 2011). Except in Paper I, we have adopted F^η -test since for all our RQWLQs, we have got comparison stars fairly close in apparent magnitude to the target object. An additional advantage of employing the F^η -test is that our results for RQWLQs can be readily compared with those available in the recent literature for other AGN

classes (Goyal et al. 2013, hereafter GGWSS13)³. A point worth emphasizing here is that while applying the F^η -test, it is specially important to use the correct rms errors on the photometric data points. It has been found that the magnitude errors returned by the routines in the data reduction softwares of DAOPHOT and IRAF, are normally underestimated by a factor η ranging between 1.3 and 1.75, as shown in various studies (e.g., Gopal-Krishna et al. 1995; Garcia et al. 1999; Sagar et al. 2004; Stalin et al. 2004b; Bachev et al. 2005). Recently Goyal et al. (2012) estimated the best-fit value of η to be 1.5. Following them, F^η -test can be expressed as :

³ Recently, de Diego (2014) has introduced an improved version of the F-test, called enhanced F-test, which includes data for several comparison stars, in order to enhance the power and reliability of the F-test. Here we have limited to the F^η -test, in order to facilitate comparison with other AGN classes, as mentioned above. The results for our entire INOV dataset for RQWLQs, based on the enhanced F-test, will be presented elsewhere.

$$F_1^\eta = \frac{\sigma_{(q-s1)}^2}{\eta^2 \langle \sigma_{q-s1}^2 \rangle}, \quad F_2^\eta = \frac{\sigma_{(q-s2)}^2}{\eta^2 \langle \sigma_{q-s2}^2 \rangle}, \quad F_{s1-s2}^\eta = \frac{\sigma_{(s1-s2)}^2}{\eta^2 \langle \sigma_{s1-s2}^2 \rangle} \quad (1)$$

where $\sigma_{(q-s1)}^2$, $\sigma_{(q-s2)}^2$ and $\sigma_{(s1-s2)}^2$ are the variances of the ‘quasar-star1’, ‘quasar-star2’ and ‘star1-star2’ DLCs and $\langle \sigma_{q-s1}^2 \rangle = \sum_{i=0}^N \sigma_{i,err}^2(q-s1)/N$, $\langle \sigma_{q-s2}^2 \rangle$ and $\langle \sigma_{s1-s2}^2 \rangle$ are the mean square (formal) rms errors of the individual data points in the ‘quasar-star1’, ‘quasar-star2’ and ‘star1-star2’ DLCs, respectively. η is the scaling factor and is taken to be 1.5 from Goyal et al. (2012), as mentioned above.

The F^η -test is applied by calculating the F values using Eq. 1, and then comparing them with the critical F value, $F_{\nu_{qs}, \nu_{ss}, \alpha}$, where α is the significance level set for the test, and ν_{qs} and ν_{ss} are the degrees of freedom for the ‘quasar-star’ and ‘star-star’ DLCs. Here, we set two significance levels, $\alpha = 0.01$ and 0.05 , which correspond to confidence levels of greater than 99 and 95 per cent, respectively. If F is found to exceed the critical value adopted, the null hypothesis (i.e., no variability) is discarded to the corresponding level of confidence. Thus, we mark a RQWLQ as *variable* (‘V’) if F -value is found to be $\geq F_c(0.99)$ for both its DLCs, which corresponds to a confidence level ≥ 99 per cent, *non-variable* (‘NV’) if any one out of two DLCs is found to have F -value $\leq F_c(0.95)$. The remaining cases are designated as *probably variable* (‘PV’).

The inferred INOV status of the DLCs of each RQWLQ, relative to two selected comparison stars, is presented in Table 3. In the first 4 columns, we list the name of the RQWLQ, date of its monitoring, duration of monitoring and the number of data points (N) in the DLC. The next two columns give the computed F values and the corresponding INOV status of the two DLCs of the RQWLQ, as inferred from the application of the F^η -test (see above). Column 7 gives the photometric error $\sigma_{i,err}(q-s)$ averaged over the data points in the ‘quasar-star’ DLCs (i.e., mean value for $q-s1$ and $q-s2$ DLCs), which typically lies between 0.02 and 0.07 mag (without the η scaling mentioned above). The last column gives the *peak-to-peak* amplitude ψ of INOV, as defined by Romero et al. (1999).

$$\psi = \sqrt{(D_{max} - D_{min})^2 - 2\sigma^2} \quad (2)$$

with $D_{min,max}$ = minimum (maximum) values in the RQWLQ DLC and $\sigma^2 = \eta^2 \langle \sigma_{q-s}^2 \rangle$, where, $\eta = 1.5$ (Goyal et al. 2012).

We have computed the INOV duty cycle (DC) for our RQWLQ sample using the definition of Romero et al. (1999),

$$DC = 100 \frac{\sum_{i=1}^n N_i(1/\Delta t_i)}{\sum_{i=1}^n (1/\Delta t_i)} \text{percent} \quad (3)$$

where $\Delta t_i = \Delta t_{i,obs}(1+z)^{-1}$ is duration of the monitoring session of a RQWLQ on the i^{th} night, corrected for its cosmological redshift, z . Since the duration of the observing session for a given RQWLQ differs from night to night, the computation of DC has been weighted by the actual monitoring duration Δt_i on the i^{th} night. N_i was set equal to 1, if INOV was detected (i.e., ‘V’ for both DLCs on the night), otherwise N_i was taken as 0.

5 RESULTS AND DISCUSSION

The present work together with Paper I & Paper II allows us to determine the INOV characteristics of RQWLQs using the entire set of 15 bona-fide RQWLQs covered in our programme launched about two years ago. This is the first investigation of the INOV properties of radio-quiet weak-line quasars and is targeted on their subset classified in the literature as good candidates for radio quiet BL Lacs. For the entire set we have got 30 DLCs which are continuous and have a duration exceeding 3.5 hours in all except one case where the duration is 3.0 hours (average duration of the 30 DLCs being 4.2 hours, see Table 4 and section 3.1). Our INOV results are based on the F^η -test, which is not only more reliable in comparison to other feasible tests (section 4), but also offers an additional advantage in that our INOV results for the RQWLQs can be directly compared with those reported in recent literature for other prominent AGN classes (see below).

The INOV results reported in Papers I & II were based on a set of 10 RQWLQs with 19 DLCs, yielding INOV duty cycle of 4 per cent. In this study, we have been able to significantly enlarge the INOV database as we now have 30 DLCs covering our entire set of 15 RQWLQs. The INOV duty cycle for the entire set is found to be ~ 5 percent (using F^η -test). In order to ascertain the effect of likely uncertainty in the adopted value of η , we have repeated the computation of INOV duty cycle for the 30 DLCs of RQWLQs, setting two extreme values for η ($= 1.3$ and 1.75) reported in the literature (Goyal et al. 2012, and references therein). The INOV DCs computed for these extreme values of η are still 5 per cent. Thus, the F^η -test is found to give a consistent result over the maximum plausible range in η .

It is interesting to compare our DC estimates for RQWLQs with those recently reported by GGWSS13 for several prominent AGN classes, again using the F^η -test with η set equal to 1.5. INOV duty cycle estimated in their study is: $\sim 10\%$ (6%) for radio-quiet quasars (RQs), $\sim 18\%$ (11%) for radio-intermediate quasars (RIQs), $\sim 5\%$ (3%) for radio lobe-dominated quasars (LDQs), $\sim 17\%$ (10%) for radio core-dominated quasars with low optical polarization (LPCDQs), $\sim 43\%$ (38%) for radio core-dominated quasars with high optical polarization (HPCDQs) and $\sim 45\%$ (32%) for BL Lac objects (BLOs) (The values inside parentheses refer to the DLCs showing INOV amplitude $\psi > 3\%$). Thus, the duty cycle of strong INOV ($\psi > 3\%$) found here for RQWLQs is similar to those reported (with $\psi > 3\%$) for RQs, RIQs, LDQs and LPCDQs, while HPCDQs and BLOs have distinctly higher duty cycle. However, this comparison is not strictly valid, given the fact that in the observations of all these other AGN classes (GGWSS13), an INOV detection threshold (ψ_{lim}) of 1–2 per cent had typically been achieved. Being 1–2 mag fainter, the INOV detection threshold reached for the present set of RQWLQs is less deep ($\psi_{lim} \approx 5$ per cent, Table 4). Thus, while making comparison with the above mentioned other AGN classes, our present estimate of INOV duty cycle for RQWLQs (~ 5 per cent) may be treated as a lower limit. This cautionary remark is underscored by the fact that both events of INOV detection reported here (Table 4) are marked by extremely large amplitudes ($\psi \sim 30\%$ peak-to-peak, occurring on hour-like time scale), rivaling blazars in their highly

active phases (e.g. Sagar et al. 2004; Gopal-Krishna et al. 2011; Goyal et al. 2012). Clearly, it would be very interesting to check if a factor of 2–3 improvement in ψ_{lim} would reveal many more events of INOV among RQWLQs, yielding a statistically robust estimate for the duty cycle of strong INOV ($\psi > 3\%$) for RQWLQs, which is distinctly higher than the present estimate of $\sim 5\%$, perhaps even approaching the high values established for blazars.

To summarize, the twin objectives pursued in our INOV study of RQWLQs are (a) to find cases of very strong INOV (ψ well above 3 per cent), any such RQWLQs would be outstanding candidates for the putative radio-quiet BL Lacs, and (b) to quantify the INOV duty cycle for RQWLQs, in both strong and weaker INOV regimes. With a significantly enlarged sample of 30 DLCs of RQWLQs in the present study, we now find that their INOV duty cycle is about 5 per cent, at a typical INOV detection threshold of around 5 per cent and a monitoring duration of about 3–5 hours. In our programme, two of the RQWLQs were found in two sessions to exhibit very strong INOV (amplitude $\psi > 10\%$), a level never observed in our 2-decade long INOV programme (summarized in GGWSS13, Goyal et al. 2012; Stalin et al. 2004b), except for BL Lacs and HPCDQs. The two RQWLQs, namely J090843.25+285229.8 ($\psi \sim 31\%$ on 10.02.2013, Table 4) and J140710.26+241853.6 ($\psi \sim 36\%$ on 03.05.2014, Figure 1, Table 4), are thus currently the best available candidates for the elusive population of radio-quiet BL Lacs and hence need to be followed up.

ACKNOWLEDGMENTS

We thank an anonymous referee for the helpful suggestions. G-K thanks the National Academy of Sciences, India for the award of Platinum Jubilee Senior Scientist fellowship.

REFERENCES

- Abazajian K. N. et al., 2009, *ApJS*, 182, 543
 Bachev R., Strigachev A., Semkov E., 2005, *MNRAS*, 358, 774
 Carini M. T., Miller H. R., 1992, *ApJ*, 385, 146
 Carini M. T., Miller H. R., Goodrich B. D., 1990, *AJ*, 100, 347
 Carini M. T., Miller H. R., Noble J. C., Goodrich B. D., 1992, *AJ*, 104, 15
 Carini M. T., Miller H. R., Noble J. C., Sadun A. C., 1991, *AJ*, 101, 1196
 Carini M. T., Noble J. C., Taylor R., Culler R., 2007, *AJ*, 133, 303
 Chand H., Kumar P., Gopal-Krishna, 2014, *MNRAS*, 441, 726(Paper II)
 Czerny B., Siemiginowska A., Janiuk A., Gupta A. C., 2008, *MNRAS*, 386, 1557
 de Diego J. A., 2010, *AJ*, 139, 1269
 de Diego J. A., 2014, *ArXiv e-prints*
 Diamond-Stanic A. M. et al., 2009, *ApJ*, 699, 782
 Elitzur M., Ho L. C., 2009, *ApJ*, 701, L91
 Garcia A., Sodr e L., Jablonski F. J., Terlevich R. J., 1999, *MNRAS*, 309, 803
 Gopal-Krishna, Goyal A., Joshi S., Karthick C., Sagar R., Wiita P. J., Anupama G. C., Sahu D. K., 2011, *MNRAS*, 416, 101
 Gopal-Krishna, Joshi R., Chand H., 2013, *MNRAS*, 430, 1302(Paper I)
 Gopal-Krishna, Sagar R., Wiita P. J., 1995, *MNRAS*, 274, 701
 Gopal-Krishna, Stalin C. S., Sagar R., Wiita P. J., 2003, *ApJ*, 586, L25
 Gopal-Krishna, Wiita P. J., Altieri B., 1993, *A&A*, 271, 89
 Goyal A., Gopal-Krishna, Wiita P. J., Anupama G. C., Sahu D. K., Sagar R., Joshi S., 2012, *A&A*, 544, A37
 Goyal A., Gopal-Krishna, Wiita P. J., Stalin C. S., Sagar R., 2013, *MNRAS*, 435, 1300(GGWSS13)
 Gupta A. C., Joshi U. C., 2005, *A&A*, 440, 855
 Heidt J., Nilsson K., 2011, *A&A*, 529, A162
 Heidt J., Wagner S. J., 1996, *A&A*, 305, 42
 Hewett P. C., Wild V., 2010, *MNRAS*, 405, 2302
 Hryniewicz K., Czerny B., Nikolajuk M., Kuraszekiewicz J., 2010, *MNRAS*, 404, 2028
 Jang M., Miller H. R., 1997, *AJ*, 114, 565
 Jannuzi B. T., Green R. F., French H., 1993, *ApJ*, 404, 100
 Joshi R., Chand H., 2013, *MNRAS*, 429, 1717
 Joshi R., Chand H., Gupta A. C., Wiita P. J., 2011, *MNRAS*, 412, 2717
 Laor A., Davis S. W., 2011, *MNRAS*, 417, 681
 Liu Y., Zhang S. N., 2011, *ApJ*, 728, L44
 Londish D., Heidt J., Boyle B. J., Croom S. M., Kedziora-Chudczer L., 2004, *MNRAS*, 352, 903
 Mangalam A. V., Wiita P. J., 1993, *ApJ*, 406, 420
 Miller H. R., Carini M. T., Goodrich B. D., 1989, *Nature*, 337, 627
 Monet D. G. et al., 2003, *AJ*, 125, 984
 Nicastro F., Martocchia A., Matt G., 2003, *ApJ*, 589, L13
 Nikolajuk M., Walter R., 2012, *MNRAS*, 420, 2518
 Paliya V. S., Stalin C. S., Kumar B., Kumar B., Bhatt V. K., Pandey S. B., Yadav R. K. S., 2013, *MNRAS*, 428, 2450
 Plotkin R. M. et al., 2010, *AJ*, 139, 390
 Romero G. E., Cellone S. A., Combi J. A., 1999, *A&AS*, 135, 477
 Sagar R. et al., 2011, *CURRENT-SCIENCE*, 101, 8
 Sagar R., Stalin C. S., Gopal-Krishna, Wiita P. J., 2004, *MNRAS*, 348, 176
 Singal K. A., Gopal-Krishna, 1985, *MNRAS*, 215, 383
 Smith P. S., Williams G. G., Schmidt G. D., Diamond-Stanic A. M., Means D. L., 2007, *ApJ*, 663, 118
 Stalin C. S., Gopal-Krishna, Sagar R., Wiita P. J., 2004a, *MNRAS*, 350, 175
 Stalin C. S., Gopal Krishna, Sagar R., Wiita P. J., 2004b, *Journal of Astrophysics and Astronomy*, 25, 1
 Stetson P. B., 1987, *PASP*, 99, 191
 Stetson P. B., 1992, in *Astronomical Society of the Pacific Conference Series*, Vol. 25, *Astronomical Data Analysis Software and Systems I*, Worrall D. M., Biemesderfer C., Barnes J., eds., p. 297
 Ulrich M.-H., Maraschi L., Urry C. M., 1997, *ARA&A*, 35, 445
 Urry C. M., Padovani P., 1995, *PASP*, 107, 803
 Wagner S. J., Witzel A., 1995, *ARA&A*, 33, 163
 Wiita P. J., 2006, in *Astronomical Society of the Pacific Conference Series*, Vol. 350, *Blazar Variability Workshop*

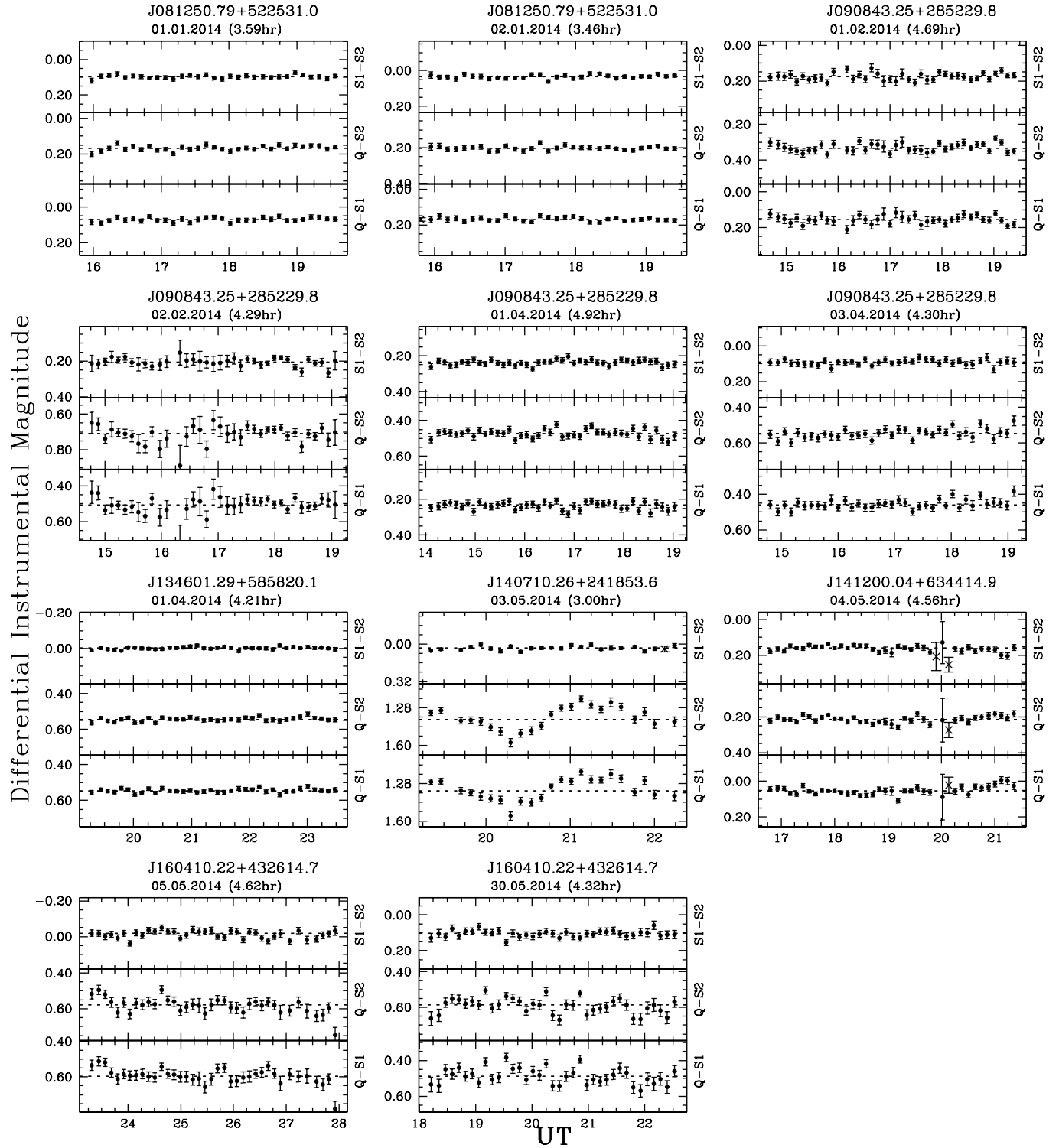


Figure 1. Differential light curves (DLCs) for the 6 RQWLQs from our sample. The name of the RQWLQ together with the date and duration of its monitoring are given at the top of each panel. In each panel the upper DLC is derived using the two non-varying comparison stars, while the lower two DLCs are the ‘quasar-star’ DLCs, as defined in the labels on the right side. Apparently outlier point (at $> 3\sigma$) in the DLCs are marked with crosses and those points have been excluded from the statistical analysis.

II: Entering the GLAST Era, Miller H. R., Marshall K.,
Webb J. R., Aller M. F., eds., p. 183
Wu J., Brandt W. N., Anderson S. F., Diamond-Stanic
A. M., Hall P. B., Plotkin R. M., Schneider D. P., Shem-
mer O., 2012, ApJ, 747, 10